

Tectonic Geomorphology of the
Toroweap Fault, western Grand
Canyon, Arizona: Implications for
Transgression of Faulting on the
Colorado Plateau

by

Garrett W. Jackson

Arizona Geological Survey Open-File Report

90-4

1990

This report is preliminary and has not been edited or
reviewed for conformity with Arizona Geological Survey
standards

GCMRC Library
DO NOT REMOVE

432.00
PRJ-10.00
J12t

<u>TABLE OF CONTENTS</u>	<u>page</u>
ABSTRACT	1
I. INTRODUCTION	2
II. PREVIOUS WORK	3
III. STUDY AREA	4
Geologic setting	4
Climatic setting	5
Quaternary geology and geomorphology	6
IV. SURFACE CLASSIFICATION	7
V. SOILS	9
Carbonate accumulation	9
Total carbonate content	11
VI. MORPHOLOGIC SCARP DATING	13
VII. ESCARPMENT SINUOSITY	17
VIII. BEHAVIOR OF THE TOROWEAP FAULT	20
Spatial variations	20
Segmentation	20
Whitmore Wash Scarps	22
Temporal variations	22
Earthquake magnitude	23
IX. IMPLICATIONS FOR TRANSGRESSION OF FAULTING	25
REFERENCES	27
APPENDIX 1. Soil profile descriptions	32
APPENDIX 2. Summary of carbonate data	34

ABSTRACT

The Toroweap fault is a major normal fault in Northwestern Arizona. Along its southern end are four displaced Quaternary surfaces, three of which have measurable displacements that are multiples of about 2.2 m. Soil carbonate analysis was carried out to estimate ages for the three surfaces. An extrapolated carbonate accumulation was used to estimate an age for the oldest surface of between 26 and 54 ka; the youngest displaced surface is between 4 and 11 ka. Oldest undisplaced surface is 2 ± 1 ka. Diffusion modelling determined the most recent surface rupture to be 3 ± 1 ka.

An aid in determining degree of tectonic activity where displaced materials are not present is the escarpment sinuosity index (Es). Escarpment length was divided by fault length. Because cliff height varies from one area to another, the index was normalized by dividing by total cliff height. The index is inversely proportional to total displacement.

Segments of the fault were distinguished using Es, presence and style of Quaternary displacements, and changes in fault orientation. There are five segments in the study area, the most active segment spanning the Grand Canyon.

This segment contains displaced basalts and alluvium, allowing estimates of displacement rates through time. The displacement rate has doubled during the Quaternary, increasing from 56 m/my to 110 m/my. This increase may be a result of the eastward migration of faulting onto the southwestern Colorado Plateau. The Toroweap Fault may be accomodating more stress with time. In addition, extrapolation of the mean Quaternary displacement rate back in time indicates that faulting began at about 4 Ma, which is much more recent than on faults to the west, which initiated movement between 6 and 10 Ma.

I. INTRODUCTION

Strikingly linear, fault-generated bedrock escarpments are common in northwestern Arizona; they define the transition between the eastern Basin and Range province and southwestern Colorado Plateau (Fig. 1). Geophysical evidence suggests that the margins of the plateau are foundering as the main body of the plateau is uplifted (Morgan and Swanberg, 1985), and that the Basin and Range province may be expanding at the expense of the Colorado Plateau (Keller and others, 1979). A widespread paucity of datable displaced materials leaves one guessing at displacement rates for much of the area.

Displacement rates can be documented for a section of the Toroweap fault in the vicinity of the Colorado River. Quaternary basalts, cinder cones, and alluvium have been faulted in Toroweap Valley on the north side of the river, and in Prospect Valley on the south side (Fig. 2). While the presence of these displacements has been known for some time, they have not been examined in detail.

With recent refinements of isotopic and geomorphologic dating techniques, an opportunity exists to a) estimate the timing and magnitude of the most recent surface rupture, b) reconstruct the Quaternary tectonic and geomorphic history of the area, and c) analyze spatial and temporal patterns of displacement on the Toroweap and other faults in the Basin and Range-Colorado Plateau transition zone.

The strategy for accomplishing these objectives involved geomorphic mapping, soil carbonate analysis, diffusion modelling of fault scarps, and measurement of escarpment sinuosity. Mapping was conducted to morphologically define displaced and undisplaced surfaces. Measurement of soil carbonate was deemed the simplest and most inexpensive method for estimating surface ages, which in turn helps constrain fault activity. Diffusion modelling was carried out to estimate the age of the most recent surface rupture. The

escarpment sinuosity index was developed as an aid in qualitatively determining fault activity in areas lacking datable materials.

II. PREVIOUS WORK

Since the late 19th century, workers have hypothesized about the behavior of the Toroweap fault, but theories have varied considerably. Powell (1875) estimated the displacement of Paleozoic rocks in the canyon at 245 m. Dutton (1882) re-examined the displacement and estimated the throw at 183-213 m. Davis (1901, 1903) proposed two episodes of movement. Johnson (1909) supported his conclusion. Moore (1925) placed the displacement in the Grand Canyon area at 155 m, but McKee and Schenk (1942) noted the succession of lavas damming Toroweap and Prospect Valleys to be 169 m above the river level. They placed "pre-lava" faulting at 148 m and "post-lava" faulting at 44.5 m, for a total 193 m. Koons (1945) devised a relative chronology of basalt flows on the Uinkaret Plateau, based on topographic position and degree of weathering. The oldest basalts were labeled "stage I" (late Miocene - Pliocene), the youngest basalts were labeled "stage IV" (latest Pleistocene-Holocene). He concluded that stage IIIb flows were displaced at least 5 to 11 m near Vulcan's Throne, and stage IIIa (early-middle Pleistocene) flows to the north had been displaced 3 to 46 m. Slightly younger stage IIIb (middle-late Pleistocene) flows in the same area are not displaced in the north, indicating cessation in, or much less frequent, fault activity.

Hamblin (1970) reclassified the basalts at Vulcan's Throne as stage IV, implying much more recent fault activity. Huntton (1977) pointed out late Quaternary movement on the Toroweap and Hurricane faults. He asserts that the maximum age of the basalt displaced in Prospect Valley is 30 ka*. He

* ka = 1000 years before present; ky = 1000 years.

recognized surface displacement in alluvium of about 6 m, and 15 m in the above basalt, indicating repeated movement. Anderson (1977), however, stated that a Holocene age assignment is not supported by the evidence that Huntoon presented. This study will show that the latest movement is indeed Holocene, but probably much older than a few hundred years, as Huntoon states.

III. STUDY AREA

Geologic setting

The area of this study spans the north and south rims of the Grand Canyon (Fig. 1), from about 50 km north of the Colorado River to Highway 66 northwest of Seligman, about 100 km from the Colorado River.

The southwestern Colorado Plateau consists of a series of fault-bounded blocks consistently downthrown to the west (Fig. 3).

The Toroweap fault is an important plateau-bounding high-angle fault. If the Aubrey and Sevier faults are considered to be part of the Toroweap fault zone (Hamblin, 1970), its total distance is over 480 km (Fig. 1a). Brumbaugh (1987) states that the southwestern Colorado Plateau is tectonically similar to the Basin and Range Province; he designated the northwesternmost part of Arizona a tectonic transition zone between the two regions. The Toroweap fault lies within this zone. Total stratigraphic displacement varies considerably along its length, however. Along the south rim of the canyon displacement is about 250 m; north of the Colorado River it decreases steadily to a few tens of meters north of Toroweap Valley. Displacement increases rapidly past this point to at least 560 m near the Arizona-Utah border. Few faults are present east of the Toroweap fault, especially south of the Colorado River; the Toroweap fault appears to be at the eastern edge of the transition zone.

The fault has a long history of activity. The earliest movement on the Toroweap fault occurred in the Precambrian, when it was a normal fault. Compression in the Laramide reactivated the fault in the opposite sense, displacing Precambrian rocks but folding the overlying Paleozoic rocks. Compression ceased in the early Tertiary and was replaced in the late Tertiary by extension. (Wenrich and others, 1986). Slickensides along several faults in the region reveal dominantly dip-slip motion (Wenrich and others, 1986).

Climatic setting

Climatically, Prospect-Toroweap Valleys are similar enough to study areas in the Great Basin and in southern New Mexico to allow extrapolation of the scarp degradation diffusivity constant and the soil carbonate accumulation rate. Most of the study area lies between 1300 m (4000 ft) and 2000 m (6000 ft) in altitude. The Aubrey Cliffs reach a maximum height of 2400 m (7315) ft, and rise abruptly up to 660 m (2000 ft) from the valley floors. The valleys are semiarid; they receive about 29 cm of precipitation each year. Winter precipitation is a few centimeters less than summer precipitation (Sellers and Hill, 1974). About 20% of winter precipitation is snow. Mean annual temperature is 14.5° C. Winters are moderately cool (average minimum January temperature is -2.5° C), while summers are warm (average maximum July temperature is 33.6° C). The southern end of Prospect Valley is somewhat cooler and more moist, because the altitude increases to 2000 m. The climate is thus broadly similar to large areas of semiarid terrain in southwestern North America.

Vegetation shows slight differences with increases in altitude. The lower altitude communities consist primarily of low grasses, yuccas, and cholla cactus. Sage, juniper, and pinon grow above about 1640 m and in protected areas at lower altitudes.

Quaternary geology and geomorphology

Prospect and Toroweap Valleys are on opposite sides of the Inner Gorge and while having similar elements, their development has differed in several important ways.

Toroweap Valley is on the north rim of the Grand Canyon, adjacent to the Uinkaret volcanic field. It is a gentle, broad valley with steep alluvial fans derived from cinder cones and lava flows on the west. Sinuous, vertical cliffs form an escarpment on the eastern side of the valley. The cliffs are deeply embayed, and fans emanating from them are broad and gently sloping. Toroweap Valley probably was once similar in form to the many adjacent tributary canyons of the Colorado River, which are generally steep, narrow, and very deep, with many lithologically controlled knickpoints and virtually no alluvium. It is likely that most of the sinuosity of the escarpment in Toroweap Valley and northern Prospect Valley, is an artifact of canyon cutting at this time, because nearby canyons display similar embayments. At about 1.2 Ma, lava began to fill ancestral Toroweap Canyon (McKee and others, 1968). Successive lava flows filled Toroweap Canyon as well as the Inner Gorge of the Grand Canyon to a level near the top of the Esplanade Sandstone, resulting in numerous dammings of the Colorado River (Rogers and Pyles, 1979, unpub. data). Since the time of extrusion of the lavas, the river has cut completely through several hundred meters of lava dams plus an additional 15.2 m through Paleozoic sedimentary rocks. River gravels at 117 m and 76 m above the river were deposited as the river cut down through the lava dams (McKee and others, 1968).

The last stage of volcanism was the emplacement of cinder cones at the mouth of Toroweap Valley. Accurate numerical ages of the cinder cones are lacking. These cinder cones, along with faulting, created Toroweap Lake, a small playa adjacent to Vulcan's Throne. The cinder cones continue to block outflowing drainage and the gradient of the axial

wash in the valley is very low. Re-incision of the former canyon is just beginning.

Prospect Valley's present form is quite different from Toroweap Valley. Lava also filled the paleocanyon of Prospect Valley (Fig. 4), presumably at about the same time that lavas filled Toroweap Canyon and the Inner Gorge. It appears that lavas filled the valley to a level perhaps 150 m below Toroweap Valley. A 30 m thick wedge of alluvial gravels was deposited in the valley, burying the basalts. These gravels overlap the remnant of a cinder cone at the head of the modern Prospect Canyon (Fig. 5), indicating that this valley was once at least partially blocked by a large cinder cone, as Toroweap Valley is today. Sediments are much thicker on the downthrown side of the fault, indicating syndepositional faulting (Fig. 6). Since then, however, the cinder cone has eroded, and a new canyon has eroded southward from the Colorado River about 1.5 km upstream from the rim of the Inner Gorge. Prospect Wash has incised completely through the Pleistocene gravels and now flows on the canyon-filling basalts. The east face of modern Prospect Canyon coincides with the fault plane. Headward erosion has proceeded along the fault to a point south of the present Prospect Wash knickpoint (Fig. 7).

Relatively steep alluvial fans emanating from the escarpment indicate that the valley floor was never as gentle as Toroweap Valley. Surfaces of various ages are more readily distinguished in Prospect Valley than in Toroweap Valley because of conspicuous differences in altitude.

II. SURFACE CLASSIFICATION

Initially, constraints on the timing of recent faulting were developed by determining relative ages of displaced and undisplaced surfaces. Four surfaces are displaced by different amounts; the youngest surface is not displaced.

This provided a framework for more detailed study and surface age estimation. Geomorphic surfaces were mapped using 1:24,000-scale aerial photographs (plates 1 and 2).

Alluvial fans, fan terraces, and stream terraces are the major landform types in the study area. "Alluvial fans", henceforth, will refer to both active fans and fan terraces, which are no longer depositional surfaces. Stream terraces are found along the axial drainages.

Systematic change of surface features with time allowed relative ages to be assigned. Young alluvial fans have bar-and-swale topography, distributary drainage, and very weak soil development. Recent debris flow paths and levees show clearly on air photos. Infilling of swales and flattening of bars occurs with time, and the surface eventually becomes very smooth where undissected by subsequent erosion. Older terraces are higher than younger terraces.

Three major stream terraces were formed in Prospect Valley. The oldest terrace, "t2", is also the highest. (Units are named by landform and relative age, eg, "t" stands for terrace and "2" is the second oldest landform.) It occupies a large area at the northern end of Prospect Valley. The thickness of the unit can be seen at the head of Prospect Canyon (see Figs. 5 & 6). "t3" is a narrow discontinuous terrace found only in the northern end of Prospect Valley. It lies 2-3 m below t2. "t4" is the youngest terrace, and lies very low in the valley, only about 1 m above the modern channel ("ch"). In some areas, t4 is dissected by arroyos that were probably cut in historic times. In these locations, t4 was the floodplain until recently.

Five distinct sets of alluvial fans were found. The oldest fan is "f1". It is found only on top of a displaced basalt flow in Prospect Valley. Surficial clasts, predominantly limestone and sandstone, are highly weathered. Minimum displacement of the flow, and therefore the surface, is about 40 m, and little of the original surface is preserved. "f2" is limited in extent as well, forming only a

few remnants close to the escarpment in Toroweap Valley, and one large fan in Prospect Valley. "f3" is considerably lower in altitude, and much more extensive. Much of the original surface is intact. Debris-flow channels and levees are clearly visible on the ground and in air photos. f3 was divided into three units to better constrain fault behavior. "f3a" is somewhat more degraded and generally occurs between the canyon mouths on the east side of northern Prospect Valley. Only subtle remnants of channels and bars are present. "f3b" is the most common subdivision (see fig.3). It has very young debris flow channels and levees. "f3c" is found in one very small area as a low cut terrace about 1 m above the modern channel. Active fans are labeled "f4"; this unit includes a complex of deposits deemed to be late Holocene by their fresh appearance and lack of soil development.

Colluvium and remnant colluvial slopes are labeled "Co₂" and "Co₁", respectively. Co₂ is found on the present face of the escarpment, and both units rest on the Hermit Shale (Fig. 3). It includes active and recently active colluvial slopes. With time, a petrocalcic horizon develops, forming a surface that armors the otherwise easily eroded Hermit Shale. Co₁ is colluvium that has formed a resistant cap on the bedrock. Dissection of the colluvium has extended to the apex of the slope, usually near the base of the Toroweap Limestone, isolating the colluvial slope from sediment input (Fig. 8). In this way, a hillslope can be "relict", representing the former position of the escarpment. Some remnants are as far as 0.75 km from the escarpment. Dating of these colluvial remnants would provide valuable information on rate of escarpment or cliff retreat.

III. SOILS

Carbonate accumulation

One strategy for estimating surface ages is using soil carbonate accumulation rates (calcium and magnesium

carbonates). Carbonate accumulation was assessed using both morphologic development of calcic horizons (Gile and others, 1966; Birkeland, 1984) and total soil carbonate (Machette, 1985).

The cliffs above Prospect Valley and Toroweap Valley are capped by limestones and dolomitic limestones, so runoff probably is rich in Ca^{++} . In addition, most of northwestern Arizona is underlain by Kaibab limestone, a probable source of eolian carbonate dust (L. Mayer, 1988, oral communication). Furthermore, the clasts of the alluvial fans are composed mostly of limestone with some limey sandstone of the Esplanade Sandstone. With these conditions, one would expect a very high rate of carbonate accumulation.

Fortunately, primary carbonate in parent material can be taken into account. No stream-bed cementation was found in modern washes, therefore runoff-precipitated carbonate is probably not significant; carbonate in soil profiles is assumed to be pedogenic.

Carbonate stage consistently increased with age of geomorphic surfaces. The maximum stage of carbonate development, stage III+ to IV- (Birkeland, 1984), was found in t₂, while f₄ had either stage I or no carbonate development. Table 3 of Machette (1985) shows age estimates of soils with the various maximum stages of carbonate morphology. But to compare Prospect Valley, we must select an area with similar climatic and geologic conditions. Fortunately, a detailed chronosequence has been studied in the Roswell-Carlsbad, N.M. area (Bachman and Machette, 1978). This area receives similar amounts of precipitation (Table 1), and seasonality is only slightly different. Temperature ranges and eolian contribution are similar. Large areas are underlain by limestone and limestone-derived alluvium, causing eolian carbonate influx to be very high; both areas have eolian contributions from large rivers, that is, the Rio Grande and the Colorado (W.B. Bull, 1990, written communication). Higher carbonate morphologic stages are

reached quickly. In the Roswell-Carlsbad area, Machette estimates that stage II begins to form after about 10 ky, and stage III forms after about 80 ky, and stage IV after about 120 ky.

Therefore, a general estimate of soil age for f4 would be 10 ka or less; for f3, between 10 and 80 ka, and for f2 between 80 and 120 ka. T2 has stage IV development (>120 ka), but appears to be graded to the f2 fan in northern Prospect Valley.

Total carbonate content

Total carbonate content may provide more precise age estimates. Machette outlined a procedure for calculating the total carbonate of a soil. The following equation is used:

$$cS = (c1)(d1)(p1) - (c3)(d3)(p3) \quad (1)$$

where:

cS = total carbonate (g/cm²)
 c1 = primary carbonate content (percent)
 d1 = initial horizon thickness (cm)
 p1 = initial bulk density (g/cm³)
 c3 = present carbonate content (percent)
 d3 = present horizon thickness (cm)
 p3 = present bulk density (g/cm³)

Primary carbonate content is assumed to be similar to the present carbonate content of unaltered C horizon (parent material). In this report, only the less than 2 mm fraction of the soil is considered. Horizon thickness is assumed to be constant, except for petrocalcic horizons, where the thickness may increase slightly with time. cS values for petrocalcic horizons are slightly higher than the actual value (Machette, 1985). Initial bulk density is also taken from the C horizon. Present carbonate content (Appendix 2) was obtained from laboratory analysis with the Chittick apparatus, using the technique described by Dreimanis (1962).

Bulk densities (p_1 and p_3) are difficult to measure in very coarse-grained alluvium. Therefore, the range of typical bulk densities was used to calculate a range of c_s . The lower limit was taken from the average of known bulk densities of soil parent material in the area, about 1.3 g/cm^3 (Soil Survey, unpub. data). A value of 2.0 g/cm^3 , typically the maximum bulk density of stage IV horizons (Machette, 1985), was used for the upper limit for p_3 in the soils with advanced carbonate morphology. For young soils, p_1 is approximately equal to p_3 . Though the original bulk density is not known, the present bulk density of parent material can be assumed to approximate it.

Carbonate accumulation rate (R_x) is not precisely known for the western Grand Canyon area. To estimate soil ages one must assume a rate calculated from an area with similar climatic and geologic conditions. Machette (1985) calculated a value for R_x of $0.51 \text{ g/cm}^2/\text{ky}$ in south-central New Mexico. Because age control is good in the Roswell-Carlsbad soils, Machette's value for R_x was used. This rate was derived from a 500 ka soil; it represents an average rate for pluvial and interpluvial periods.

Age estimates for soils in Prospect Valley using c_s show good agreement with age estimates from surface morphology and correlated carbonate stages (Table 2). The oldest surface analyzed, T2, is estimated at $80 \pm 30 \text{ ka}$. f2 ranges from 26 to 54 ka. f3b ranges from 4 to 11 ka, averaging 7.5 ka. The two ages estimates for t4 and f4, the youngest surfaces, are both just over 2 ka. The ages for the older surfaces probably represent underestimates of the actual ages, since the development of stage IV usually doesn't begin until about 100 ka, and f2 has local, spotty occurrences of this stage. The age obtained for f3c is older than geomorphic relations indicate. This may be attributed to the location of described profile. The stream-cut exposure showed a gentle swale that may have been filled mostly by eolian dust. This would greatly enhance carbonate development.

There are several potential sources of error in these age estimates. First, one must accept the extrapolated carbonate accumulation rate. The similarity of soil-forming conditions in Prospect Valley and Roswell-Carlsbad make this extrapolation possible. Second, bulk densities are assumed. However, using the range of possible bulk densities still yields useful results. Third, detrital carbonate particles less than about 1 mm in diameter were included in the calculation of carbonate percentage. The fourth, and most important limitation is that carbonate rinds on clasts were not taken into account. Therefore the age estimates would be minima. At least part of the carbonate found on the undersides of limestone clasts is simply re-precipitated from the limestone clasts themselves. Preliminary data from K.R. Vincent (written communication, 1990) indicate that carbonate rinds contribute at most 40%, but probably 20% of total carbonate. This means that the ages may be underestimated by a maximum of 40%, and probably by about 20%.

The surface ages estimated indicate that the most recent faulting occurred before the deposition of f4 and T4 at about 2 ka, and after 4-11 ka. Because f2 is displaced significantly more than f3b, at least two surface-rupturing events have occurred during the last 50 ka or so.

IV. MORPHOLOGIC SCARP DATING

Scarps in alluvium allow more precise constraint of the age of the last surface rupture (Bucknam and Anderson, 1979). Scarps are present from where the fault leaves basalt flows in central Toroweap Valley to southern end of Prospect Valley, near the Prospect graben (see fig. 11).

Scarp degradation can be modelled as a diffusion process (Nash, 1980, 1984 ; Colman and Watson, 1983 Hanks and others, 1984). The diffusion modelling technique is based on the assumptions of linear mass transport downslope and conservation of mass. The basic form of the diffusion equation is:

$$dy/dt = k(d^2y/dx^2) \quad (2)$$

In terms of geomorphic processes, equation (2) means that the change in altitude at a point with time is proportional to the rate of change of slope at that point. The constant k is referred to as "diffusivity", and in this use represents the complex interaction of climate, vegetation and lithology (meaning clast sizes and sorting). Important assumptions of the model are 1) that the scarp is a closed system, 2) that the movement of material is transport-limited (more material is available to transport than the transportational processes operating on the slopes can move), and 3) that the rate of movement of material downslope is directly proportional to the slope. These assumptions are reasonable for scarps cut in unconsolidated to weakly consolidated alluvium and when profiles are carefully selected.

The stages in the evolution of a scarp are shown in Figure 9. Initially, a fresh scarp has a near vertical free face. Mass wasting accompanied by sheetwash and raindrop splash soon lowers the free face to the angle of repose (Wallace, 1977). In unconsolidated alluvium, this process happens as fast as two weeks, and at several localities has happened in less than 100 years (K.L. Pierce, unpub. data), which is a short period of time compared to the age of the scarp. Therefore the time it takes for the scarp to reach the angle of repose can be neglected. After that, erosional processes behave according to the diffusion model.

The procedure developed by Nash (1984) was used to estimate scarp ages. In this method, measured scarp parameters are substituted into the solution of the diffusion equation. The computer program SLOPEAGE, also developed by Nash, greatly facilitated calculations. The angle of repose, measured on recent stream cuts, was $34^\circ \pm 1^\circ$. Profiles perpendicular to the strike of the scarps were surveyed in the field using two techniques. The first involves using a

flat measuring stick and a compass with an inclinometer. The slope angle and distance are measured in successive increments, moving up the scarp. The second method is preferable because it is much faster; it requires two people and uses a measuring tape and an inclinometer. The tape is stretched between the two people at the same height above the ground. One person looks upslope to the other person and records the angle, sitting on the same height above ground (eye height of the person sitting) each time. Profiles measured with both techniques at the same site are very similar.

Ideally, an independently dated scarp is used to calculate a site-specific value of diffusivity. However, there are no dated scarps in the study area. An established value must be taken from an area of similar climate and lithology. Hanks and others (1984) showed that a diffusivity of $1.1 \text{ m}^2/\text{ky}$ could be used on fault scarps throughout the Great Basin. However, diffusivity has been shown to increase with scarp height (Pierce and Colman, 1986). Fortunately, single-rupture scarps on the Toroweap are generally between about 1 m and 4 m in height. Scarp height in this range has only a small effect on diffusivity. Ideally, a locally derived regression of diffusivity on height, with independent age control, should be used. In west-central Nevada, Demsey (1987) used this technique and found that ages derived from a locally-derived equation for k were only slightly different from those using the regional value for k of $1.1 \text{ m}^2/\text{ky}$. It should be possible to estimate age of surface rupture on the Toroweap fault scarps using $1.1 \text{ m}^2/\text{ky}$ for diffusivity, since the climate and materials in Prospect Valley are similar to those of piedmont scarps in the Great Basin (P.A. Pearthree, 1989, oral communication).

Results of the analysis are summarized in Table 3. In Prospect Valley 43 profiles were surveyed. Only 34 of these were used for age estimates; the rest were suitable only for determining the amount of displacement, due to scarp

complexity. Alluvium in Prospect Valley is more similar to the alluvium for which the diffusivity of $1.1 \text{ m}^2/\text{ky}$ was developed than alluvium in Toroweap Valley. Dividing tk by $1.1 \text{ m}^2/\text{ky}$ yields an estimate of $3.1 \pm 1.6 \text{ ka}$. This is consistent with the estimated soil age for f3b (4-11 ka), which provides a maximum age of rupture, and with the age range of f4 ($2 \pm 1 \text{ ka}$), which is not displaced.

Fourteen profiles were measured in Toroweap Valley. Eight of these were used for age estimates. Average tk , the age of rupture times the diffusivity constant, is $18.14 \pm 3.52 \text{ m}^2$ for Toroweap Valley. The average tk is $3.5 \pm 1.8 \text{ m}^2$, for Prospect Valley.

The difference in tk values between the two valleys may be explained by significant differences in clast size of alluvium. In Toroweap Valley, the displaced alluvium is generally no larger than pebble size, and is predominantly composed of fine gravel and sand. Prospect Valley, on the other hand, has alluvial fans with very coarse clasts, ranging from sand to house-size boulders, but generally in the cobble size range. The two sets of scarps are very different in morphology due to these differences in clast size. Dodge and Grose (1980) show that fault scarps produced by the same event can appear very different. Figure 10a, from their paper, shows on a log scarp height vs. scarp slope angle graph the effect of clast size on scarp slope angle.

Figure 10b shows that the separation of the regression lines of height vs. slope age for the Prospect-Toroweap scarps is similar to what Dodge and Grose found. In addition, the regression lines are parallel, indicating that the scarp-producing events occurred at the same time.

The Inner Gorge of the Grand Canyon leaves several kilometers of scarp missing between the two valleys. While it is possible that some surface ruptures did not cross the Inner Gorge, it is likely that the scarps were formed by the same event. In addition, there is no evidence for fault

segmentation at the Inner Gorge, such as structural salients or a change in fault strike.

V. ESCARPMENT SINUOSITY

Transition-zone faults typically do not cut or lack Quaternary deposits and even much of the Toroweap fault lacks Quaternary fault scarps. An additional geomorphic analysis was needed to evaluate degree of tectonic activity in these areas. The sinuosity of bedrock escarpments along the Toroweap fault was evaluated for these purposes.

The degree of erosion of the faulted surface is a geomorphic feature useful for assessing relative tectonic activity. This type of indicator compares a present form with the initial, fault-generated form. It represents the balance between forces that degrade the landform (eg., stream incision, mass-wasting) and forces that renew the landform, namely continued faulting.

Modification of fault-generated mountain fronts by erosion may be quantified. Bull and McFadden (1977) used stream-valley morphology and mountain-front sinuosity. The latter property is perhaps the most easily used. It involves measuring the length of mountain front-piedmont boundary and dividing by the length along the fault to get a sinuosity index. The index shows the degree of degradation from the original, more planar form of the mountain front.

The sinuosity of fault-generated bedrock escarpments can be used in a similar manner. However, bedrock escarpments have morphologic properties different from Basin-and-Range mountain fronts that must be considered.

Escarpments have 1) nearly vertical cliffs on the fault-bounded side, 2) a resistant capping layer, and 3) a subplanar crest.

Retreat of escarpments from the fault tends to be slow, relative to the rate of mountain-front retreat. Furthermore, the subplanar surface on the upthrown side, if dipping away from the fault (typical in northwestern Arizona), diverts

stream flow away from the escarpment and escarpment sinuositities tend to be relatively low compared to mountain-front sinuositities.

Escarpments have a relatively resistant capping layer. The resistance to erosion of this layer may vary considerably with different lithologies. Fortunately, most of the escarpments in northwestern Arizona are capped by the Kaibab Formation, a very resistant limestone (see Fig. 3).

Embayment seems to be the main form of escarpment modification. Parallel retreat or slope replacement may take place depending on the location of the drainage divide (Mayer, 1986), but either way, continued development of drainage basins on the escarpment face will produce embayments. As streams incise into the escarpment, the junction between the escarpment and the valley floor increases in length. Conversely, when the fault ruptures, the junction decreases in length.

Factors affecting drainage-basin development affect escarpment sinuosity, and should be taken into account. Cliff orientation, altitude, and height are the most important. Orientation of escarpments on the southwestern Colorado Plateau are generally NNW to NNE, and can be assumed constant. Altitude of the escarpment affects precipitation and vegetation. An escarpment with a crest at 1000 m is likely to receive less precipitation, and thus will degrade more slowly, than an escarpment with a crest at 2000 m. Fortunately, most escarpment crests in the area lie at 1700-2100 m. Cliff height does vary considerably within the area studied, and was taken into account in the calculation of the escarpment sinuosity index:

$$Es = [(E_1/F_1) - 1]/Ch \quad (3)$$

where: Es = escarpment sinuosity index
 E_1 = escarpment length
 F_1 = fault length

C_h = cliff height

The length of the base of the Toroweap escarpment was measured along the most prominent break in slope, using a map wheel and 1:24,000 scale topographic maps. The length of the fault could in many places be measured directly from the map of the fault trace, and in the other areas was inferred to within probably less than 100 m. Because the quotient of the two lengths is greater than or equal to one, one was subtracted to make the minimum value zero. This was divided by the cliff height, measured by the difference in altitude between the crest of the escarpment and the fault trace.

The fault was divided into segments 3-7 km in length. The length of the segments depended on the curvature of the fault; where the fault makes sharp bends, the segments are 1-3 km long. The two segments that cross two large embayments, Crater Canyon and Rhodes Canyon (see fig.2) show index values that are not representative of the area. In this case, the index was averaged by adding adjacent segments into the calculation. The lengths of the escarpment-piedmont junction for the three adjacent segments were totaled and divided by the sum of the fault-trace lengths. The quotient was then divided by the weighted average cliff height.

Es values are quite low, as expected (Fig. 11). Several segments have indices less than 0.10. In these cases, the differences between the escarpment length and the fault length were beyond the resolution of the map wheel used. These segments indicate relatively greater tectonic activity, or more rapid uplift, than in segments with higher sinuosity indices.

A check on the sinuosity index is presented in Figure 11. Total displacement (from Huntton, and others, 1981, 1983, and Billingsley and others, 1986) is plotted along the length of the fault. Sinuosity index is plotted on the distances to the midpoint of the segments along the fault. This figure shows that where displacement is high, Es is low,

and where it is low, E_s is high. This demonstrates that sinuosity does describe the relative activity of the fault, assuming that where displacement is high, displacement is rapid.

V. BEHAVIOR OF THE TOROWEAP FAULT

Three aspects of fault behavior can be analyzed with the information in this study: spatial variation, temporal variation, and earthquake magnitude.

Spatial variations

Segmentation

It is apparent from stratigraphic displacement that significant variation in displacement rates occurs along the Toroweap fault (see Fig. 11). Escarpment sinuosity, along with stratigraphic displacement and estimated displacement rates in Toroweap Valley and northern Prospect Valley allow the fault to be divided into segments of different relative tectonic activity. These segments are shown by the large letters in Figure 2.

Segment A is relatively inactive. Escarpment sinuosity index is high, $30 \times 10^{-3} \text{ ft}^{-1}$. In addition, f3 has not been displaced. No clear displacement is evident in the basalts, which are probably early to mid-Pleistocene in age. Total displacement is less than 76 m (Huntoon and others, 1981), which also suggests a very low long-term displacement rate.

The boundary between segment A and segment B is gradational, occurring over about 5 km. Segment B has been the most active part of the fault, at least during the Quaternary. Total displacement ranges from 150 to 265 m, varying locally as other structures intersect the fault (see Fig. 11). Sinuosity index is very low, except where the effects of pre-lava incision are present. Displacement rates range from 56 m/my to 100 m/my. At least three surface-rupturing events have occurred in the latest Quaternary. The

boundary with the next segment is gradational, occurring over about 7 km.

Segment C is a short segment characterized by low sinuosity indices, but has no visible Quaternary displacements. Total displacement, 280 m, is the highest anywhere on the Toroweap fault in Arizona. This segment may be as active as segment B; evidence for recent activity may be lacking or obscured due active colluvial slopes and thick vegetation.

The fault bends 90° to the east at the southernmost part of Prospect Valley, where segment D begins. East of the bend, stratigraphic throw rapidly decreases to about 54 m. No evidence of Quaternary fault activity exists in segment D. Though many alluvial fans and terraces cross the fault, none are displaced and sinuosity is relatively high, being about $4.0 \times 10^{-3} \text{ ft}^{-1}$. At a point about 5 km west of Frazier's Well, the escarpment becomes very sinuous and almost nonexistent, forming a series of low hills rising gently to the northeast. No displacements in Quaternary alluvium are present. Although Huntton and others (1981) found displaced landslides of late Tertiary to early Quaternary age, mapping by Billingsley and others (1986) show only Tertiary-age Frazier's Well gravels to be displaced. Total displacement of Paleozoic strata is 122 m.

About 10 km east of Frazier's Well, another 90° bend returns the fault to a north-south orientation. At this point, displacement increases again, reaching as much as 213 m. From here to just north of Seligman, where the Aubrey Cliffs rise abruptly to 488 m, is segment E. Total displacement at Crater Canyon is about 137 m. Quaternary alluvium has been displaced in the vicinity of Rhodes Canyon. Here there are relatively steep fault scarps (P.A. Pearthree, unpub. data). These scarps were modelled using the diffusion equation and an average age of 4.9 ka is obtained, using a diffusivity of $1.1 \text{ m}^2/\text{ky}$. This would make the rupture very close in age to the rupture in Prospect Valley. With recent

scarps and low sinuosity indices, segment E appears to be moderately active, much like segment B. In addition, a small closed depression containing a playa, indicative of active normal faulting, exists at the base of the escarpment. The length of segment E is about 45 km, which is as long as Segment B.

Whitmore Wash Scarps

About eight kilometers west of the Toroweap fault, in Whitmore Wash, early Holocene fault scarps can be found along the Hurricane Fault. Average displacement, measured from 8 profiles, is 2.8 ± 0.7 m. Scarp profiles (P.A. Pearthree, unpub. data) were modelled, revealing k of 8.8 ± 3.7 m². Assuming 1.1 m² is applicable for k , age of rupture is about 8 ± 3 ka.

Temporal variations

Given an age range of 26-54 ka for surface f2, and an average displacement of 2.2 m per event (fig. 12), it seems that at least three ruptures have occurred since the late Pleistocene. Two events occurred between the formation of f2, at about 40 ka, and the most recent event, at about 3 ka. The actual displacement rate is the difference in total displacements of f2 and f3b divided by the difference in ages, which gives a minimum rate of 0.11 ± 0.02 m/ky, or 110 ± 20 m/my.

The estimated displacement rate since 40 ± 14 ka (110 m/my) is substantially higher than the rate determined from a displaced basalt. This basalt is in northern Toroweap Valley and is displaced 36 m. An age of 635 ± 24 ka was determined by K/Ar methods, indicating an average displacement rate of 56 m/my. Near Vulcan's Throne, a basalt displaced 15 m was dated at 203 ka (Anderson and Christensen, 1989), giving a minimum displacement rate of 74 m/my. which is intermediate between the rates discussed above. Assuming no significant lateral change in displacement rate within the segment, these

rates for different time intervals suggest that the Toroweap fault is accommodating more stress with time.

Longer term displacement rates are even lower. Inception of faulting in this part of the Colorado Plateau is poorly constrained. Normal faulting in southwestern Utah began about 8-10 Ma (Anderson and Mehnert, 1979), while the main phase of faulting in the Lake Mead area was 6-10 Ma (Hamblin and Best, 1970; Lucchitta, 1979). To the southwest of segment E, the main phase of Basin and Range style faulting was between 8 and 10 Ma (McKee and Anderson, 1971). The Hurricane fault, as close as 8 km to the west of the Toroweap fault, did not begin normal movement until the Miocene. Total displacement of Paleozoic rocks at the Grand Canyon is about 193 m; if 8-10 Ma is assumed as the beginning of movement on the Toroweap fault, an average displacement rate of 16-24 m/my is obtained.

Earthquake Magnitude

Another characteristic of faulting that can be estimated is the magnitude of surface-rupturing events. To do this, the average surface displacement must be measured in the field. Because the surface area of the fault plane is proportional to the seismic source moment, the following equation can then be used to get the moment (Brune, 1968 ; Hanks and Kanamori, 1979):

$$M_0 = u v A \quad (4)$$

where:

- M_0 = seismic source moment
- u = crustal rigidity
- v = average surface displacement
- A = fault plane area

Fault plane area is a product of length of rupture (L), depth of faulting (d) and the down-dip distance of the fault plane

(f). Therefore, the moment can be calculated using the modified equation:

$$M_0 = \frac{u \cdot v \cdot d \cdot L}{\sin \phi} \quad (5)$$

where: ϕ = dip of fault plane in degrees

because: $f = d/\sin \phi$.

The seismic source moment is related to magnitude by :

$$M_w = 2/3 \log M_0 - 10.7 \quad (6)$$

where M_w = moment magnitude
(Hanks and Kanamori, 1979).

Use of these equations requires four assumptions: 1) fault scarp displacements represent a single earthquake, 2) strain is accommodated by faulting alone, 3) rigidity of the crust is about 3.3×10^{11} dyne/cm², and 4) the depth of faulting is about 15 km (T.C. Wallace, 1989, oral communication). The assumptions seem reasonable given the preservation of the scarp, lack of drag structures or brecciation (McKee and Schenk, 1942). Because the dip of the fault is close to vertical, $d \sim f$.

The length of rupture could not be determined exactly, due to erosion of scarps or transition into bedrock scarps. Instead, a range of rupture length was identified based on last occurrence of displaced alluvium and the first appearance of unfaulted f3 alluvium. The rupture length was between 53 and 62 km. Moment magnitude ranged between 7.1 and 7.2.

Another way of estimating paleoearthquake magnitudes is not dependent on depth to faulting or surface displacement. This uses surface-wave magnitude, which approximates M_w for $M < 8.0$. Equation (7) relates surface wave magnitude to rupture length and stress drop, which is about 100 bars for

the Colorado Plateau (T.C. Wallace, 1989, oral communication):

$$M_s = (\log L + 2.1 + 2/3 \log \Delta s) \ 3/2 \ (7)$$

where: M_s = surface wave magnitude

Δs = stress drop

Magnitude ranges from 7.7 to 7.8, which is significantly higher than magnitudes estimated with the other method. With either method, it is clear that earthquakes along the Toroweap fault are strong enough to cause significant damage.

VII. IMPLICATIONS FOR MIGRATION OF FAULTING

If the rate of displacement along the Toroweap fault is increasing modestly with time (Fig. 13), it supports hypotheses that invoke the progressive breakup of the margins of the Colorado Plateau (Wong and Humphrey, 1986; Morgan and Swanberg, 1985; Keller and others, 1979; Hamblin and Best, 1975). Migration of faulting has been documented in other areas of the Colorado Plateau's margins.

In south-central Utah, Rowley and others (1981) showed that faulting shifted uniformly from the Basin and Range (9 Ma) to the Sevier fault (7.6-5.4 Ma) to the Paunsagaunt fault (<5 Ma). Hamblin and others (1981) show that in southwestern Utah, the rate of displacement across major normal faults increased to the east from the plateau's physiographic boundary.

In the western Grand Canyon area, faulting seems to be migrating diffusely to the east, while western faults become less active. Estimated Quaternary displacement rates on the Toroweap fault presented in this paper show moderate increases with time (Fig. 13). In addition, escarpment sinuosity, shown to be inversely related to fault activity, decreases from west to east. The Grand Wash cliffs are highly embayed and sinuous (Mayer, 1986), indicating

relatively low displacement rates. In fact, no movement has occurred on the Grand Wash fault since almost 11 Ma in the area south of Pearce's Ferry (Lucchitta, 1979). Although some movement has occurred to the north of Lake Mead, fault scarps are limited in extent and are poorly constrained in age, being designated less than 500 ka. Farther north, near the Virgin Mountains, the last movement was probably during the Pliocene (Menges and Pearthree, 1983). Mapping by Huntoon and others (1981, 1983) has shown that faults lying between the Grand Wash and Toroweap faults, with the exception of the Hurricane fault in Whitmore Wash, have not displaced Quaternary units, where present. One major fault, the Dellenbaugh fault (see Fig. 1), does not displace a Pliocene basalt. This indicates that either faulting has ceased or that recurrence intervals are very long.

Best and Hamblin (1975) estimate that faulting has migrated eastward at 10 km/my, and that volcanism has migrated 30 km/my eastward (Best and Hamblin, 1978). However, Menges (1983) suggests that migration of faulting in northwestern Arizona is more diffuse than in southwestern Utah, involving "diachronous faulting in a large band". The recent faulting on both the Hurricane and Toroweap faults indicates that no single eastern fault is taking up the present displacement, which supports this hypothesis. The locus of faulting apparently has passed through the Shivwits Plateau (see fig. 1b) and to the east toward the Hurricane and Toroweap faults. Figure 13 shows that faulting on the Toroweap fault may have begun at about 4 Ma, if the Quaternary displacement rate is extrapolated back through time. This is significantly later than the main phase of faulting in the areas adjacent to the Colorado Plateau margin (6-10 Ma). If faulting on the western plateau is assumed to have begun synchronously with the adjacent areas, the displacement rate has increased substantially in the Quaternary; this may also be interpreted as the encroachment of Basin-and-Range-style faulting.

Billingsley and others (1986) point out a young, fault-bounded depression to the east of the Aubrey cliffs. This feature, along with low magnitude seismic activity in the eastern Grand Canyon area (Brumbaugh, 1986), may represent continued migration of faulting.

REFERENCES

- Anderson, C.A., 1971, Age and chemistry of Tertiary volcanic rocks in north-central Arizona and relation of the rocks to the Colorado Plateau, Geol. Soc. Am. Bull. v.82, p. 2767-2782.
- Anderson, R.E., and Christensen, G.C., 1989, Quaternary faults, folds and related volcanic features of the Cedar City 1' X 2' Quadrangle, Utah; Utah Geological and Mineralogical Survey Misc. Paper 89-6, 29p.
- Anderson, R.E., and Huntton, P.W., 1979, Holocene faulting in the western Grand Canyon, Arizona; discussion and reply: Geol. Soc. Am. Bull. v.90, n.2, p.1221-1224.
- Anderson, R.E., and Mehnert, H.H., 1979, Reinterpretation of the history of the Hurricane fault in Utah; in Basin and Range Symposium, Newman, G.W., and Goode, H.D., eds.: Rocky Mountain Association of Geologists, p.145-166.
- Bachman, G.O., and Machette, M.N., 1977, Calcic soils and calcretes in the southwestern United States: U.S. Geological Survey Open-file report 77-794, 163p.
- Best, M.G., McKee, E.H., and Damon, P.E., 1980, Space-time composition patterns of late Cenozoic mafic volcanism, southwestern Utah and adjoining areas: Am. Jour. Sci. v.280 p.1035-1050.
- Billingsley, G.H., Wenrich, K.J., and Huntton, P.W., 1986, Breccia pipe and geologic map of the southeastern Hualapai Indian Reservation and vicinity, Arizona; U.S., Geological Survey Open-File Report 86-458B.
- Birkeland, P.W., 1984, Soils and geomorphology, New York: Oxford University Press; 372p.
- Blissenbach, E., 1952, Geology of the Aubrey south of the Hualapai Indian Reservation, Northwestern Arizona: Plateau, v.24, n.4, p.119-127.

- Brune J.N., 1968, Seismic moment, seismicity and rate of slip along major fault zones: *Journal of Geophysical Research*, v.75, n.2, p.777-784.
- Bucknam, R.C., and Anderson, R.E., 1979, Estimation of fault scarp ages from a scarp height-slope angle relationship: *Geology*, v.7, p.11-14.
- Bull, W.B., and McFadden, L.D., 1977, Tectonic geomorphology north and south of the Garlock Fault, California, in *Geomorphology in Arid Regions*, Doehring, D.O., ed., *Publications in Geomorphology*, State University of New York at Binghamton, p.115-138.
- Colman, S.M., and Watson, K., 1983, Ages estimated from a diffusion model for scarp degradation: *Science*, v.221, p.263-265.
- Damon, P.E., 1965, Correlation and chronology of ore deposits and volcanic rocks: *Arizona Univ. Geochronology abs. Ann. Prog. Report*. C00-689-50, 157 p.
- Davis, W.M., 1901, An excursion to the Grand Canyon of the Colorado: *Harvard Univ. Museum of Comparative Zoology Bulletin*, v.38, p.107-201.
- Davis, W.M., 1903, An excursion to the Plateau Province of Utah and Arizona, *Harvard Univ. Museum of Comparative Zoology Bulletin*, v. 34, p.135-161.
- Demsey, K., 1987, Holocene faulting and tectonic geomorphology along the Wassuk Range, west-central Nevada; unpub. master's manuscript, University of Arizona, 64p.
- Dodge, R.L., and Grose, L.T., 1980, Tectonic and geomorphic evolution of the Black Rock fault, Northwestern Nevada; in *Earthquake hazards along the Wasatch-Sierra Nevada frontal fault zones*, Andrise, P.C., ed., *U.S. Geological Survey Open File Report 80-801*, p.494-508.
- Dreimanis, A., 1962, Quantitative determination of calcite and dolomite by using Chittick apparatus: *Journ. of Sed. Pet.*, v.32, n.3, p.520-529.
- Dutton, C.E., 1882, *The Tertiary history of the Grand Canyon District*: U.S.G.S. Monograph #2.
- Gile, L.H., Peterson, F.F., and Grossman, R.B., 1966, Morphological and genetic sequences of carbonate accumulation in desert soils: *Soil Science*, v.101, p.347-360

- Hamblin, W.K., 1970, Structure of the western grand Canyon region, in Hamblin, W.K., Best, M.G., eds., The western grand Canyon district: Utah Geol. Soc. Guidebook to the Geology of Utah, n.23, p.21-37.
- Hamblin, W.K., and Best, M.G., 1970, The western Grand Canyon district; Guidebook to the geology of Utah, n.23; Salt Lake City: Utah Geological Society; 155p.
- Hamblin, W.K., and Best, M.G., 1975, Origin of the northern Basin and Range Province: implications from the geology of its eastern boundary: in Smith, R.B., and Eaton, G.P., eds., Cenozoic Tectonics and Regional Geophysics of the western Cordillera; Geol. Soc. Am. Memoir 152, p.313-340.
- Hamblin, W.K., Damon, P.E., and Bull, W.B., 1981, Estimates of vertical crustal strain rates along the western margins of the Colorado Plateau: Geology, v.9, p.293-298.
- Hanks, T.C., Bucknam, R.C., Lajoie, K.R., Wallace, R.E., 1984, Modification of wave-cut and fault-controlled landforms, Jour.Geophys.Res., V.89 b7, p.5771-5790.
- Hanks, T.C., Kanamori, H., 1979, A moment magnitude scale: Jour.Geophys.Res., V.84, p.1619-1622.
- Harden, J.W., 1982, A quantitative index of soil development from field descriptions: examples from a chronosequence in central California: Geoderma, V.28, p.1-28.
- Harden, J.W., and Taylor, E.M., 1983, A quantitative comparison of soil development in four climatic regimes: Quaternary Research, v. 20. p.342-359.
- Huntoon, P.W., 1977, Holocene faulting in the western Grand Canyon, Arizona, Geol. Soc. Am. Bull., V.88, p.1619-1622.
- Huntoon, P.W., Billingsley, G.H., and Clark, M.D., 1981, Geologic map of the Hurricane Fault Zone and vicinity, western Grand Canyon, Arizona; Grand Canyon, Arizona: Grand Canyon Natural History Association, 1:48,000.
- _____, 1983, Geologic map of Vulcan's Throne and vicinity, western Grand Canyon, Arizona; Grand Canyon, Arizona: Grand Canyon, Arizona: Grand Canyon Natural History Association, 1:48,000.
- Johnson, P.W., 1909, A geological excursion to the Grand Canyon district: Boston Society of Natural History Proceedings, v.34, p.135-161.

- Keller, G.R., Braile, L.W., and Morgan, P., 1979, Crustal structure, geophysical models and contemporary tectonism of the Colorado Plateau; *Tectonophysics* v.61, p.131-147.
- Koons, E.D., 1945, Geology of the Uinkaret Plateau, northern Arizona: *Geological Soc. America Bull* v.56, p.151-180.
- Koons, E.D., 1964, Structure of the Eastern Hualapai Indian Reservation: *Arizona Geological Society Digest*, .7, p.97-114.
- Lucchitta, I., 1979, Late Cenozoic uplift of the southwestern Colorado Plateau and adjacent lower Colorado River region; *Tectonophysics* v.61, p.63-95.
- Machette, M.N., 1985, Calcic soils of the southwestern United States: *in* *Soils and Quaternary Geology of the Southwestern United States: Geological Soc. America Special Paper 203*; p.1-22.
- Mayer, L., 1979, Evolution of the Mogollon Rim in central Arizona; *Tectonophysics*, v.61, p.49-62.
- _____, 1986, Tectonic geomorphology of escarpments and mountain fronts, *in* *Active Tectonics*; Washington: National Academy Press, p.125-135.
- McKee, E.D., and Schenk, E.T., 1942, The lower Canyon lavas and related features at Toroweap in the Grand Canyon: *Journal of Geomorphology*, V.5, p.97-114.
- McKee, E.D., Wilson, R.F., Breed, W.J., and Breed, C.S. (eds.), 1967, *Evolution of the Colorado River in Arizona*. *Mus. North. Ariz. Bull.* 44: 67p.
- Menges, C.M., and Pearthree, P.A., 1983, Map of neotectonic (latest Pliocene-Quaternary) deformation in Arizona; Arizona Bureau of Geology and Mineral Technology Open File Report 83-22, 1:500,000, 21 p.text.
- Menges, C.M., 1983, The neotectonic framework of Arizona: implication for the regional character of Basin-Range tectonism, Arizona Bureau of Geology and Mineral Technology Open File Report 83-19, 109p.
- Moore, R.C., 1925, Geologic report on the Inner Gorge of the Grand Canyon of the Colorado River, U.S.G.S. Water supply paper 556, p.125-171.
- Morgan, , P., and Swanberg, C.A., 1985, On the Cenozoic uplift and tectonic stability of the Colorado Plateau: *Journal of Geodynamics*, V.3, p.39-63.

- Nash, D.B., 1980, Morphologic dating of degraded normal fault scarps: *Journal of Geology*, v.88, p.353-360.
- Nash, D.B., 1984, Morphologic dating of fluvial terrace scarps and fault scarps near West Yellowstone, Montana: *Geol. Soc. Am. Bull.*, v.95, p.1413-1424.
- Pierce, H.W., Damon, P.E., and Shafiqullah, M., 1979, An Oligocene (?) Colorado Plateau edge in Arizona; *Tectonophysics* v.61, p.1-24.
- Reynolds, S.J., 1988, *Geologic Map of Arizona*; Tucson: Arizona Geological Survey; 1:1,000,000.
- Rowley, P.D., Steven, T.A., and Mehnert, H.H., 1981, Origin and structural implications of upper Miocene rhyolites in Kingston Canyon, Piute County, Utah; *Geol. Soc. Am. Bull.*, p.1, v.92, p.590-602.
- Sellers, W.D., and Hills, R.H., 1974, Arizona Climate; Tucson: University of Arizona Press, 450p.
- Sowers, J.M., Reheis, M.C., and Taylor, E.M., 1988, Soil development as a function of time, in Sowers, J.M., ed., *Geomorphology and Pedology on the Kyle Canyon alluvial fan, southern Nevada*; *Geol. Soc. Am. Field Trip Guidebook, Cordilleran Section Mtg.*
- Powell, J.W., 1875, Exploration of the Colorado River of the West and its tributaries, 1869-1872, Smithsonian Institute, Washington, D.C.
- Wallace, R.E., 1977, Profiles and ages of young fault scarps, north central Nevada: *Geological Society of America Bulletin*, v.88, p.1267-1281.
- Wenrich, K.J., Billingsley, G.H., and Huntoon, 1986, Breccia Pipe and Geologic Map of the Northwestern Hualapai Indian Reservation and vicinity, Arizona; U.S. Geol. Survey Open File Report 86-458-C
- Wong, I.G., and Humphrey, J.R., 1986, Seismotectonics of the Colorado Plateau, *Geol. Soc. Am. Abstracts with Programs* v.12 n.5, p.424.

Soil/ surface	Horizon	thickness	color (dry)	color (moist)	texture	structure	dry consist.	%>2mm
2/f2	Av	0-15	5YR 5/4	5YR 4/6	7c 75s	m sgl grn	lse	5
	AB	15-50	5YR 5/4	5YR 4/4	9c 75s	mod fm cmb	sft	10
	Bk	50-104	5YR 7/3	5YR 5/4	15c 60s	wk m sbk	shd	55
	C		2.5YR 6/6	2.5YR 4/6	4c 80s	m sgl grn	lse	65
4/ch	Av	0-20	5YR 6/6	5YR 4/8	4c 83s	wk m sbk	sft	10
	C		5YR 6/6	5YR 4/6	3c 85s	sgl grn	lse	70
5/f2	A	0-20	5YR 6/3	5YR 4/4	10c 73s	m sgl grn	lse	3
	Bk	20-75	5YR 7/3	5YR 5/4	17c 55s	mod mc cmb	hd	40
	BC	75-140	5YR 6/4	5YR 4/6	20c 55s	mod m cmb	shd	65
	C1	140-185	5YR 6/4	5YR 4/4	13c 65s	sgl grn	shd	65
6/f2	Av	0-18	7.5YR 6/4	7.5YR 4/6	15c 65s	mod m cmb	sft	30
	Bk1	18-25	5YR 7/3	5YR 5/4		stg c abk	ehd	60
	Bk2	25-57	5YR 7/4	5YR 5/6	7c 80s	stg m abk	hd	70
	Bk3	57-114	5YR 6/4	5YR 5/6	5c 85s	wk f cmb	sft	75
	C		2.5YR 5/6	2.5YR 4/6	3c 90s	m sgl grn	lse	65
7/f2	Av	0-9	7.5YR 5/4	7.5YR 4/4	5c 50s	wk m pty	sft	30
	A2	9-38	5YR 6/4	5YR 4/4	12c 50s	mod m sbk	shd	30
	Bk1	38-103	5YR 6/4	5YR 4/6	20c 50s	mod m sbk	hd	50
	Ck		5YR 6/4	5YR 5/4	7c 70s	sgl grn	lse	70
8/f2	A	0-25	5YR 5/4	5YR 4/4	10c 80s	wk m cmb	sft	30
	Bk1	25-35	2.5YR 7/3	2.5YR 5/6	15c 85s	stg abk	vhd	50
	Bk2	35-85	2.5YR 7/3	2.5YR 5/6	15c 85s	wk m abk	shd	55
	BC	85-150	5YR 6/4	5YR 5/6	8c 85s	mod m abk	shd	45
	C		5YR 6/4	5YR 4/6	7c 88s	wk f cmb	lse	50
9/f4	Av	0-15	5YR 5/4	5YR 3/4	7c 85s	mod m cmb	sft	40
	AB	15-65	5YR 5/4	5YR 3/4	10c 85s	wk c cmb	sft	40
	Bw	65-95	7.5YR 6/4	7.5YR 4/6	5c 90s	wk f sbk	sft	70
	C		5YR 5/6	5YR 3/6	5c 95s	sgl grn	lse	60
10/T4	A	0-4	5YR 5/4	5YR 4/4	5c 87s	wk m pty	sft	3
	Bw	4-45	5YR 5/6	5YR 3/6	15c 50s	mod m cmb	sft	3
	C1	45-75	5YR 5/6	5YR 3/6	15c 50s	mod mc cmb	shd	5
	C2		5YR 6/4	5YR 5/4	3c 90s	sgl grn	lse	60
11/f3b	A	0-20	5YR 6/4	5YR 4/4	4c 85s	sgl grn	lse	30
	Bw	20-75	2.5YR 6/4	2.5YR 4/6	7c 85s	wk f cmb	sft	35
	C1	75-110	2.5YR 6/6	2.5YR 4/6	3c 87s	sgl grn	lse	55
	C2		2.5YR 6/6	2.5YR 4/6	5c 85s	wk c abk	hd	30
12/f3b	A	0-27	7.5YR 5/4	7.5YR 4/4	10c 75s	wk c cmb	sft	25
	Ck		5YR 6/4	5YR 5/6	5c 80s	sgl grn	lse	60
13/f3b	Av	0-20	5YR 5/4	5YR 3/4	12c 75s	wk m cmb	sft	25
	AB	20-45	5YR 6/4	5YR 4.4	10c 80s	wk m cmb	sft	50

	Bk	45-83	5YR 6/4	5YR 5/6	10c 83s	wl m sbk	sft	50
	Ab	83-106	5YR 5/4	5YR 4/4	10c 75s	wk m cmb	sft	45
	Cb		5YR 6/6	5YR 4/8	10c 65s	sgl grn	lse	55
14/f3b	A	0-19	5YR 5/4	5YR 3/4	12c 75s	wk c cmb	sft	25
	C		2.5YR 6/6	2.5YR 4/6	5c 80s	msv	sft	30
15/f3b	Av	0-27	5YR 5/4	5YR 4/4	12c 70s	wk f cmb	sft	35
	Ck1	27-74	2.5YR 6/6	2.5YR 5/6	8c 80s	wk m cmb	sft	55
	2Ck		5YR 6/4	5YR 4/6	5c 85s	wk f cmb	sft	80
16/T2	Av	0-5	5YR 5/4	5YR 4/4	10c 75s	wk c cmb	sft	20
	A2	5.-53	5YR 5/4	5YR 4/4	15c 75s	wk m sbk	shd	30
	Bk1	53-93	5YR 8/3	5YR 6/4		st mc abk	vhd	40
	Bk2	93-153	5YR 6/4	5YR 5/6	5c 90s	mod m sbk	hd	55
	Bk3	153-233	5YR 6/4	5YR 5/4	3c 80s	wk m sbk	shd	75
	Ck		5YR 6/6	5YR 4/6	3c 80s	sgl grn	lse	75
17/f3b	Av	0-25	5YR 5/4	5YR 4/4	7c 80s	wk m pty	sft	25
	Bk1	25-65	5YR 7/4	5YR 5/6	15c 65s	stg m abk	shd	30
	Bk2	65-83	5YR 6/4	5YR 4/4	5c 80s	wk m abk	shd	60
	C		5YR 5/6	5YR 4/4	5c 80s	sgl grn	lse	50
18/f3b	A	0-26	5YR 4/4	5YR 3/4	10c 80s	wk c cmb	sft	30
	Bw	26-54	5YR 6/4	5YR 4/6	15c 80s	mod m abk	shd	50
	C		5YR 5/6	5YR 4/8	3c 80s	msv	shd	30
22/f3a	A	0-19	7.5YR 4/3	7.5YR 3/3	10c 80s	sgl grn	lse	20
	Bt	19-43	7.5YR 4/3	7.5YR 2/3	25c 40s	wk m sbk	shd	15
	Btk	43-65	7.5YR 5/3	7.5YR 3/4	15c 50s	wk m sbk	shd	30
	Bk	65-92	7.5YR 6/2	7.5YR 4/3	5c 85s	wk m sbk	hd	65
	Ck		5YR 5.5/4	5YR 4/4	7c 85s	sgl grn	lse	65

Appendix 2. Summary of carbonate data

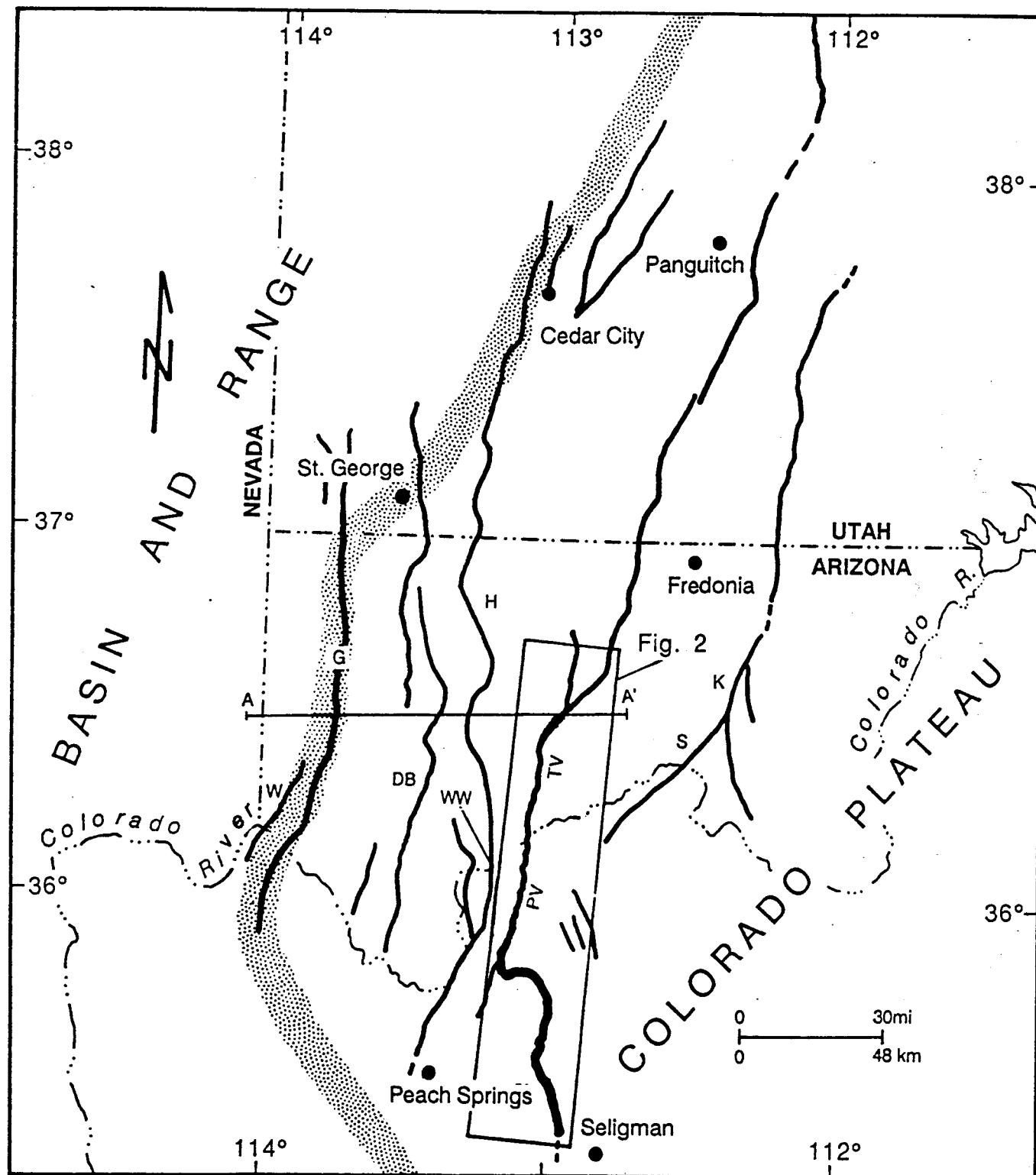
34

Soil/ surface	Horizon	maximum carbonate stage	carbonate content (percent)	total carbonate content (cS) (g/cm ²)	estimated age (ka)
2/f2	Av	IV-	17.6	13.5	26.5
	AB		29.5		
	Bk		18.9		
	C		13.9		
4/ch	Av	-	-	-	-
	C		-		
5/f2	A	II+	41.5	27.4	53.7
	Bk		40.9		
	BC		31.0		
	C1		27.9		
6/f2	Av	IV-	-	-	-
	Bk1		-		
	Bk2		-		
	Bk3		-		
	C		-		
7/f2	Av	II+	-	-	-
	A2		-		
	Bk1		-		
	Ck		-		
8/f2	A	III+	18.3	22.5	44.1
	Bk1		72.2		
	Bk2		32.5		
	BC		20.7		
	C		17.2		
9/f4	Av	I	13.0	1.1	5.3
	AB		15.8		
	Bw		25.2		
	C		15.8		
10/T4	A	-	17.8	1.2	2.4
	Bw		19.9		
	C1		18.4		
	C2		-		
11/f3b	A	II-	18.7	2.2	4.3
	Bw		24.2		
	C1		19.5		
	C2		-		

13/f3b	Av	I	-	-	
	AB				
	Bk				
	Ab				
	Cb				
14/f3b	A	-	11.3	-	-
	C		15.4		
15/f3b	Av	I	9.0	-	-
	Ck1		31.1		
	2Ck		-		
16/T2	Av	IV	8.0	41.1	80.6
	A2		11.3		
	Bk1		69.3		
	Bk2		28.3		
	Bk3		16.4		
	Ck		15.1		
17/f3b	Av	III-	8.9	5.4	10.7
	Bk1		42.1		
	Bk2		29.9		
	C		17.3		
18/f3c	A	II	5.4	4.6	9.0
	Bw		36.3		
	C		11.2		
22/f3a (?)	A	II+	23.3	3.7	7.2
	Bt		11.8		
	Btk		52.1		
	Bk		22.5		
	Ck		22.5		

Figure 1a. Location map with selected normal faults. Stipple pattern shows the approximate physiographic boundary between the Colorado Plateau and the Basin and Range provinces. GW = Grand Wash fault; T = Toroweap fault (including Sevier and Aubrey faults); D B = Dellenbaugh fault; H = Hurricane fault; W = Wheeler fault. PV = Prospect Valley; TV = Toroweap Valley; WW = Whitmore Wash area. Scale 1:1,900,800. After Hamblin and Best (1975), and Reynolds (1988).

Figure 1b: Cross-section of the western Colorado Plateau (after Hamblin and Best, 1975). QTb = Tertiary and Quaternary basalts; Tb = Tertiary basalts. Each fault has an associated escarpment.



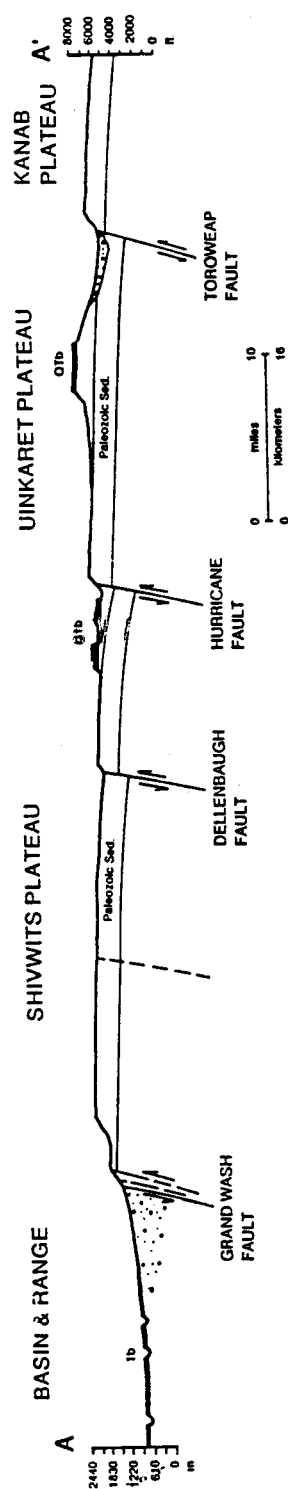


Figure 2. Map of study area. Large letters are segments of the fault. Dashed lines separate segments. RC = Rhodes Canyon; CC = Crater Canyon; FW = Frazier's Well. Box enclosed the mapped area. Hatchures indicate part of the fault for which escarpment sinuosity indices were calculated.

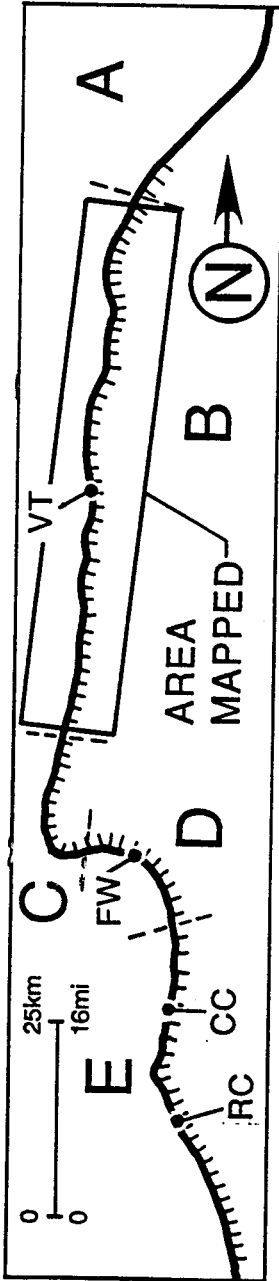


Figure 3. View of features in northern Prospect Valley. Escarpment-forming units: k = Kaibab Formation; t = Toroweap Formation; c = Coconino Sandstone; h = Hermit Shale; e = Esplanade Sandstone; s = Supai Formation. Alluvial units: f4, f3b, t4; see text for discussion. Arrows point to recent fault scarp.

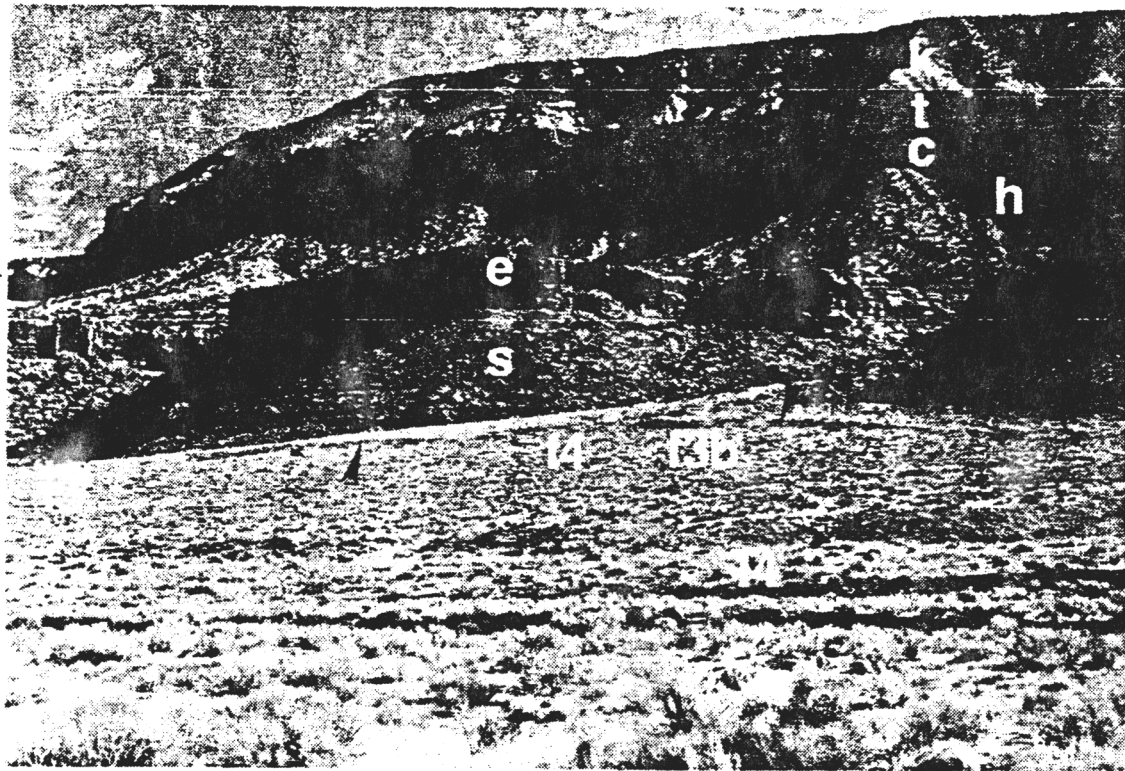


Figure 4. View of Prospect Valley, looking south from the north rim of the Grand Canyon. The Inner Gorge of the canyon is in foreground. Prospect Canyon (center) has eroded along the Toroweap fault, cutting through Quaternary basalts and cinder cones that filled a previous canyon. The Toroweap-Aubrey Cliffs (left and on the horizon) consist of two escarpments here. The upper, snow-covered cliffs are capped by the Kaibab Formation. The lower cliffs are capped by the Esplanade sandstone. The fault is at the base of the lower cliffs. The occurrence of two escarpments is unique to the northern 10 km of Prospect Valley and is probably related to pre-lava canyon incision.

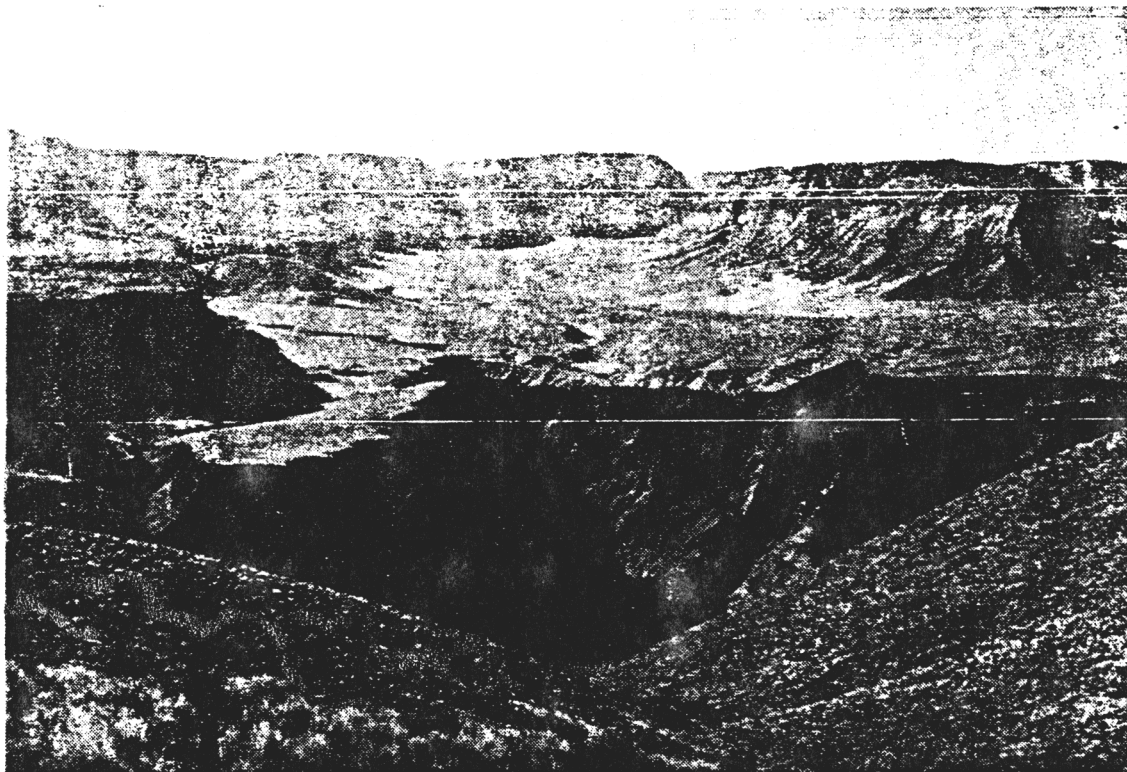


Figure 5. View looking south from Vulcan's Throne into Prospect Valley. Alluvium (center) is deposited on canyon-filling basalts and is about 30 m thick.. The alluvium also overlies the southern end of the cinder cone on the right. This cinder cone probably blocked the ancestral Prospect Valley. Prospect Wash is to the left.

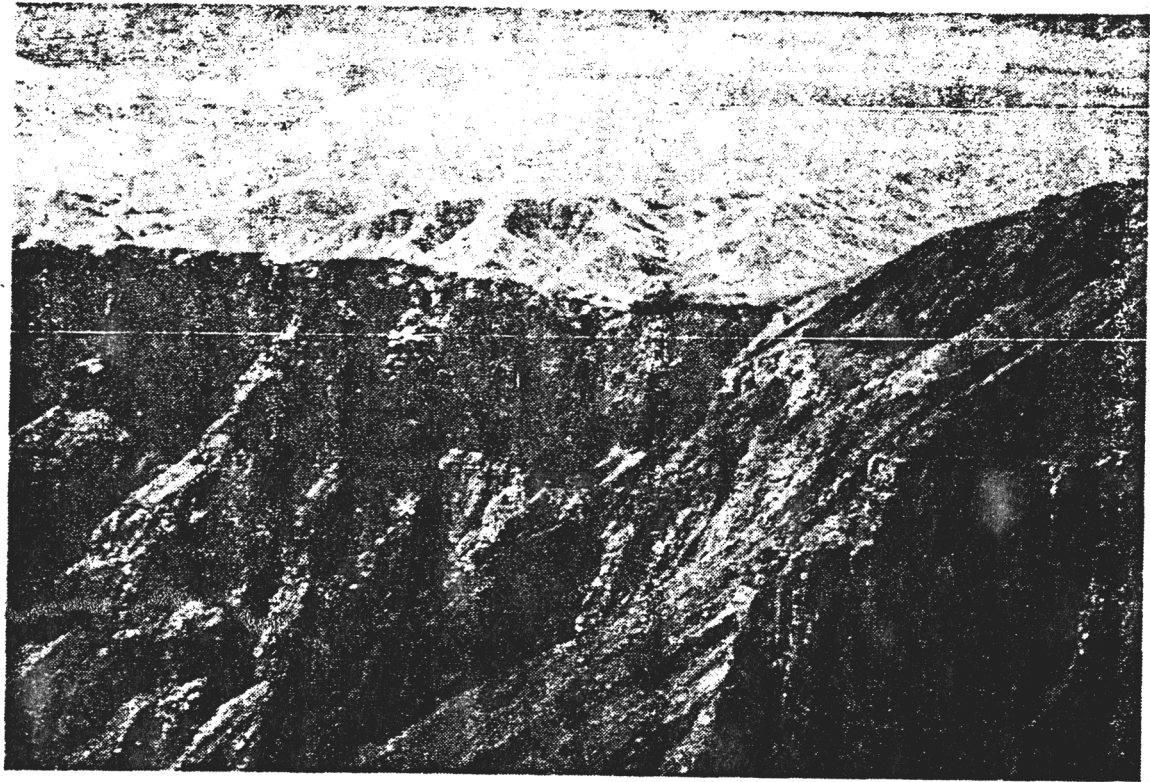


Figure 6. View of displaced North Wash basalt (oblique to fault plane). Alluvium is much thicker on the downthrown side (right) than on the upthrown side (left). Displacement of basalt, measured with tape and inclinometer, is about 65 m. Two fault strands are visible (arrows) in the center of the photo. Associated scarps can be seen in the profile of the ridge in the center.



Figure 7. View looking west from top of Esplanade escarpment. Prospect Canyon (center) has eroded past Prospect Wash, creating a 400 m knickpoint. Cinder cone (right) appears to be cut by this incision. Removal of the cinder cone, which ponded alluvium, allowed Prospect Wash to incise. It is now flowing on canyon-filling basalt.

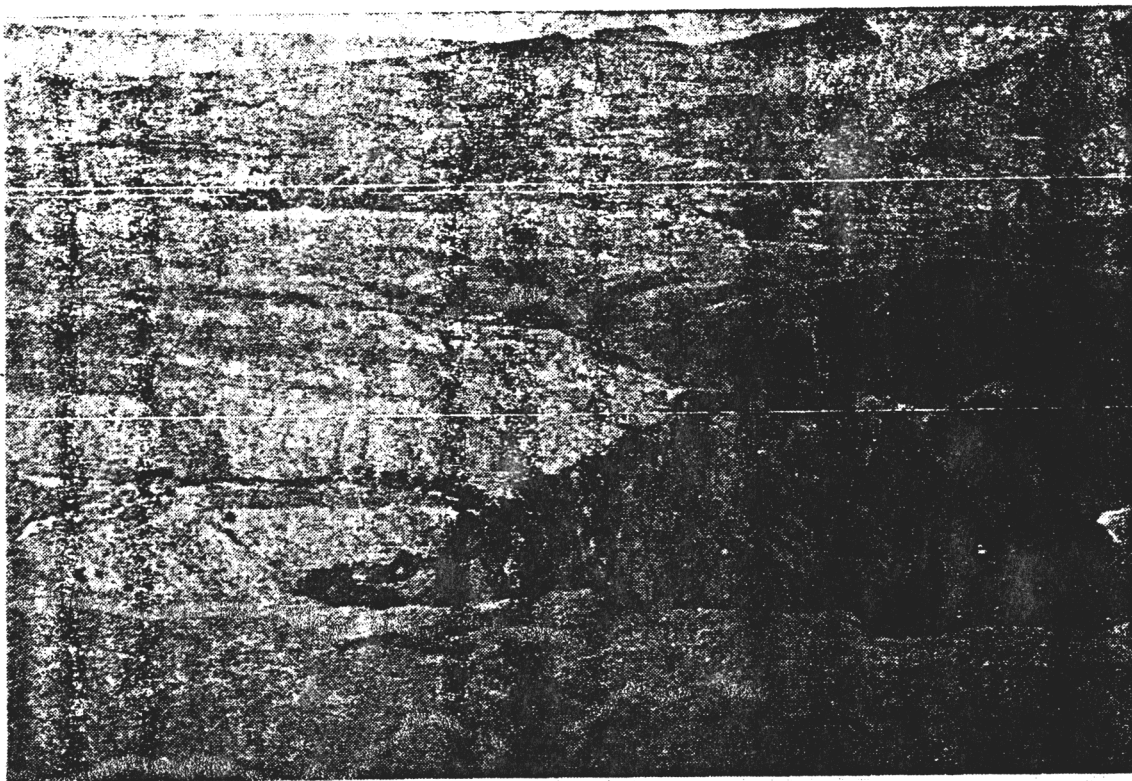


Figure 8. Co₁ is shown on the skyline, to the right (arrow). Limestone colluvium with a petrocalcic horizon has formed a resistant capping over the friable Hermit Shale. Undercutting has removed surrounding material. The top of this hillslope may represent the former position of the high cliffs to the left. Fault is at the base of the lower cliffs in the center of the photograph.



Figure 9. Idealized evolution of a single-event fault scarp. 0 = initial state after rupture, with free face being greater than the angle of repose of the material. 1 = after scarp has raveled, with the material at the angle of repose ($\sim 35^\circ$). 2 = thousands of years later, after diffusion-type processes have rounded the scarp crest and built up the colluvial wedge at the base. 3, 4 = subsequent degradation of the scarp, with the profile resembling the error function. Vertical exaggeration 2X.

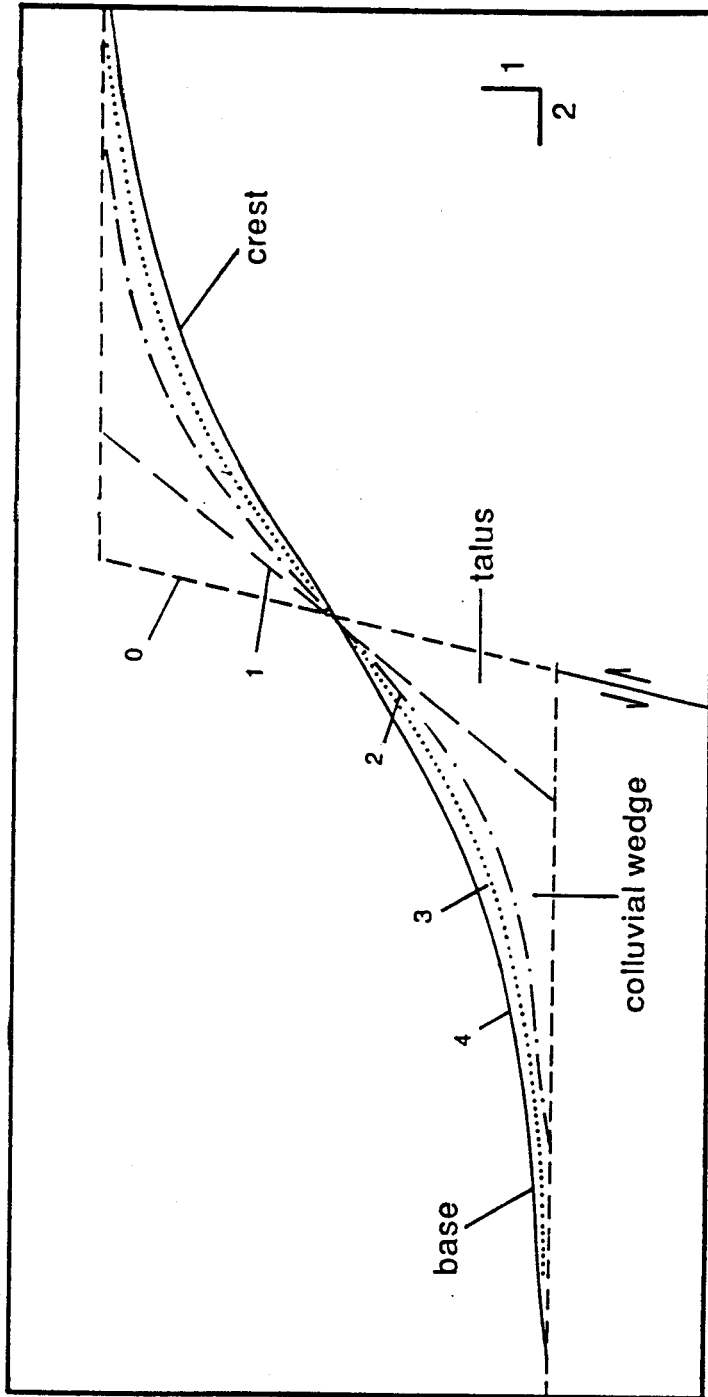


TABLE 1. Comparison of climate and soil formation conditions, Toroweap-Prospect Valleys and Roswell-Carsbad, New Mexico. Climatic data from National Oceanic and Atmospheric Administration (1981) and Sellers and Hills (1974).

<u>PARAMETER</u>	<u>Toroweap-Prospect Valleys</u>	<u>Roswell-Carlsbad</u>
Mean annual temperature	14.5	15.1
Mean annual precepitation	28.9	26.9
Parent Material	Limestone gravels	Limestone gravels
colian dust sources	Limestone bedrock; Colorado River	Limestone bedrock and gravels; Rio Grande River

Table 2. Comparison of age estimates using different techniques. *correlated to Roswell-Carlsbad, N.M. (Machette, 1985). **Carbonate accumulation rate of $0.63 \text{ g/cm}^2/\text{ky}$ from Roswell-Carlsbad, N.M. (Machette, 1985).

Surface	age ranges from corre- lated carbonate stage (ka)*	age estimate from total carbonate (ka)**
f4, T4	0-10	2 ± 1
f3c	--	--
f3b	10-80	4-11
f3a	--	--
f2	80-120	26-54
T2	120-500	80 ± 30
f1	--	--

Table 3. Summary of diffusion modelling results

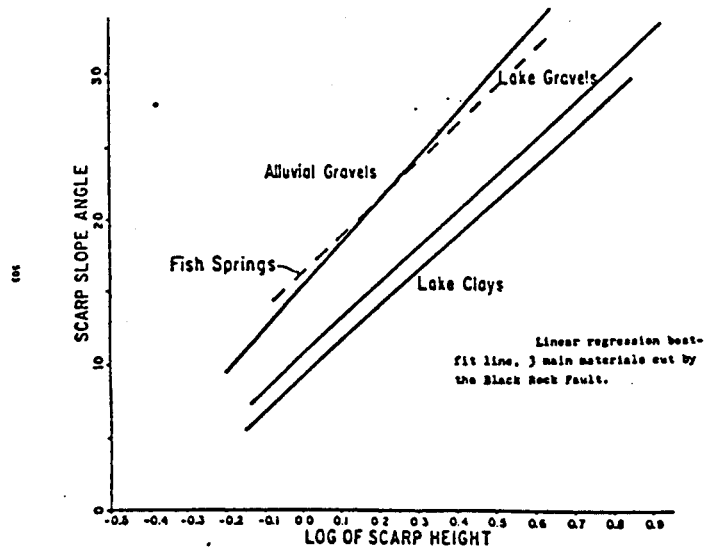
Location and surface ¹	Parameter ²	Numerical values		
		Mean	Standard deviation	Sample size
Prospect Valley				
f3(b)	D (m)	2.5	± 1.6	n=43
	tk (m^2)	3.5	± 1.8	n=39
	t (ky)	3.1	± 1.6	n=39
f2	D (m)	6.6	± 1.5	n=9
co2 and f3a	D (m)	4.4	± 0.2	n=10
Toroweap Valley				
f3	D (m)	2.1	± 0.3	n=8
	tk (m^2)	16.4	± 3.0	n=8
	t (ky)	15.0	± 2.8	n=8
Both valleys				
f3 and f3(b)	D (m)	2.2	± 0.9	n=47

¹ see fig. 1 for location and text for surface definitions

² D = displacement; t = age of rupture; k = diffusivity

Figure 10. a: Scarp slope angle vs. log scarp height plots for three different different materials (from Dodge and Grose, 1980). Fine grained material tends to make the scarps appear older than in poorly sorted alluvial gravels. b: Comparison of slope-height plot for Prospect and Toroweap Valley scarps. In Toroweap Valley scarps are in fine distal fan sediments, whereas in Prospect Valley scarps are in very coarse, proximal sediments. Sub-parallel regression lines indicate all other factors, including time, are similar.

a:



b:

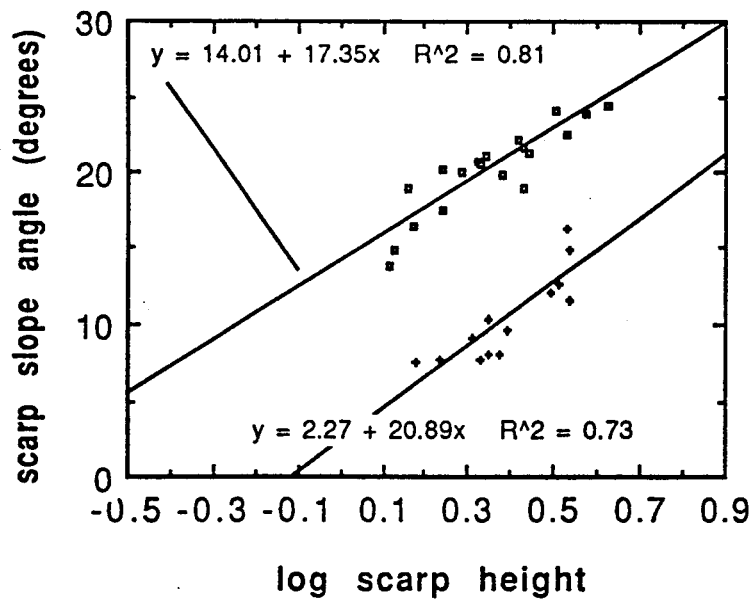


Figure 11. Variation in total displacement and sinuosity index (E_s) along the length of the Toroweap-Aubrey fault. Sinuosity is low where displacement is high and high where displacement is low. This is most likely a reflection of long-term uplift rates, which are inversely proportional to sinuosity indices. Distances are north (positive) and south (negative) of Frazier's Well. Capital letters indicate the various segments of the fault. Displacement data are from Huntton and others (1981, 1983), Billingsley and others (1986), and Blissenbach (1952).

Total displacement and sinuosity index (Es)
along the Toroweap Fault

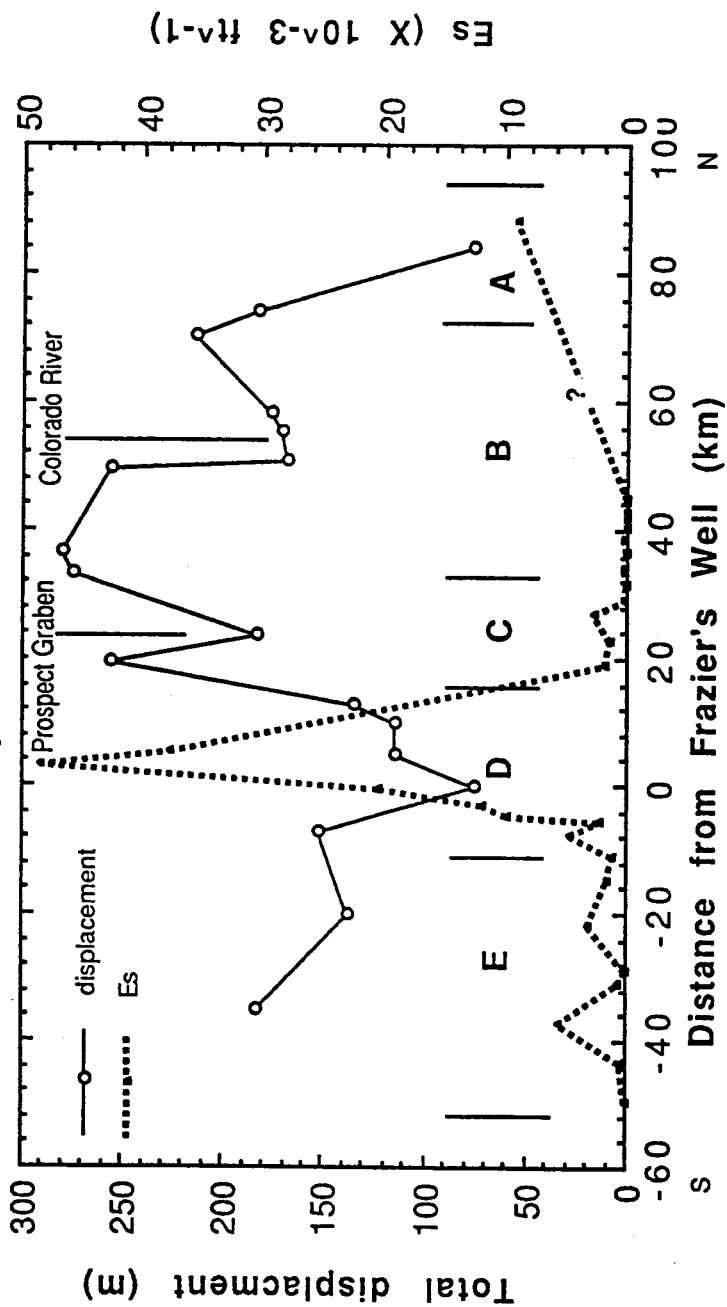


Figure 12. Average amount of displacement for three surfaces. Displacement for f2 and f3a is from PV; displacement for f3b is from both TV and PV. Typical displacement for each event is about 2.2 m.

Average displacements for three surfaces in Propect and Toroweap Valleys

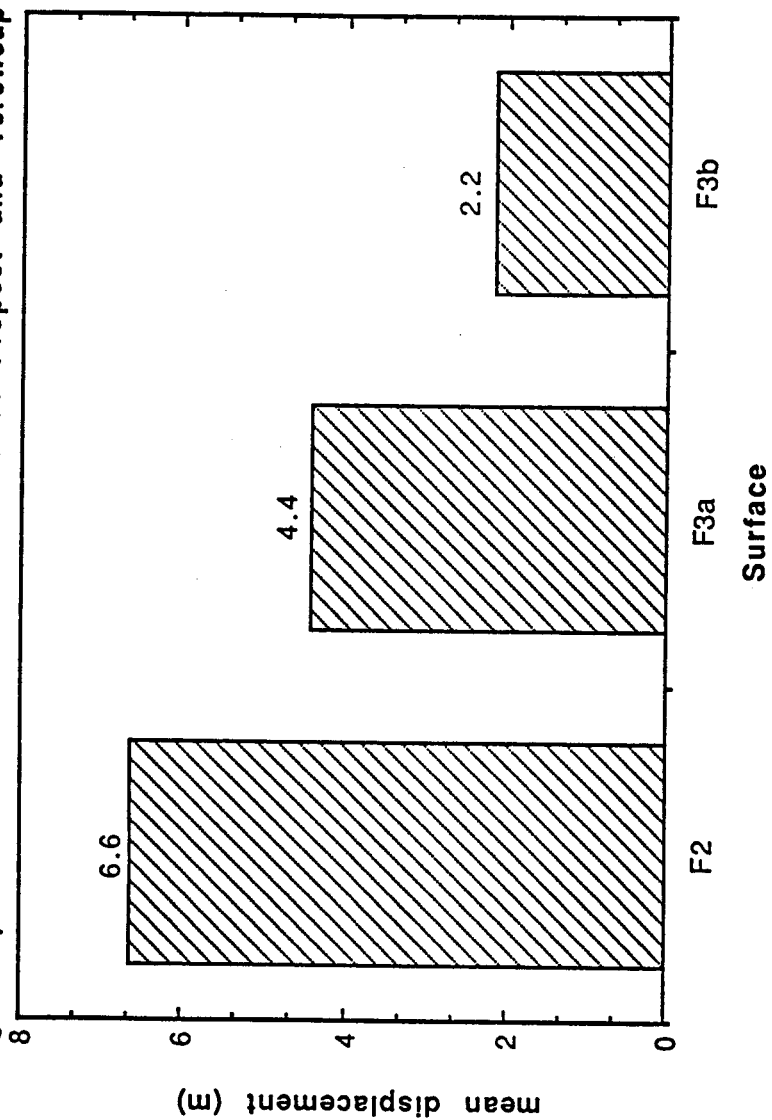


Figure 13. Variation in displacement with time. Dashed line shows extrapolated late Quaternary displacement rate. This suggests that either the rate has dramatically increased during the Quaternary, or that faulting began much more recently than previously thought. Either conclusion suggests encroachment of Basin-and-Range-style tectonism onto the Plateau during the latest Cenozoic. TV = Toroweap Valley basalt; VT = Vulcan's Throne basalt; f2 = f2 surface; R = regional inception of faulting, displacement at the Colorado River.

